

# The sealing and lubrication principles of plain radial lip seals : an experimental study of local tangential deformations and film thickness

**Citation for published version (APA):**

Leeuwen, van, H. J., & Wolfert, M. A. (1997). The sealing and lubrication principles of plain radial lip seals : an experimental study of local tangential deformations and film thickness. In C. M. Taylor, T. H. C. Childs, D. Dowson, A. A. Lubrecht, & G. Dalmaz (Eds.), *Elastohydrodynamics '96 : fundamentals and applications in lubrication and traction : proceedings of the 23rd Leeds-Lyon symposium on tribology, held at the Institute of Tribology, department of Mechanical Engineering, University of Leeds, UK, September 10-13, 1996* (pp. 219-232). (Tribology series; Vol. 32). Elsevier.

**Document status and date:**

Published: 01/01/1997

**Document Version:**

Accepted manuscript including changes made at the peer-review stage

**Please check the document version of this publication:**

- A submitted manuscript is the version of the article upon submission and before peer-review. There can be important differences between the submitted version and the official published version of record. People interested in the research are advised to contact the author for the final version of the publication, or visit the DOI to the publisher's website.
- The final author version and the galley proof are versions of the publication after peer review.
- The final published version features the final layout of the paper including the volume, issue and page numbers.

[Link to publication](#)

**General rights**

Copyright and moral rights for the publications made accessible in the public portal are retained by the authors and/or other copyright owners and it is a condition of accessing publications that users recognise and abide by the legal requirements associated with these rights.

- Users may download and print one copy of any publication from the public portal for the purpose of private study or research.
- You may not further distribute the material or use it for any profit-making activity or commercial gain
- You may freely distribute the URL identifying the publication in the public portal.

If the publication is distributed under the terms of Article 25fa of the Dutch Copyright Act, indicated by the "Taverne" license above, please follow below link for the End User Agreement:

[www.tue.nl/taverne](http://www.tue.nl/taverne)

**Take down policy**

If you believe that this document breaches copyright please contact us at:

[openaccess@tue.nl](mailto:openaccess@tue.nl)

providing details and we will investigate your claim.

## The sealing and lubrication principles of plain radial lip seals: an experimental study of local tangential deformations and film thickness

Harry van Leeuwen and Marcel Wolfert  
Eindhoven University of Technology, Dept. of Mechanical Engineering,  
P.O. Box 513, 5600 MB Eindhoven, Netherlands

Tangential deformations of the seal surface at the contact zone between a shaft and a radial lip seal are determined by image analysis of video camera pictures. These displacements are thought to be essential for the sealing mechanism. The results show that all seals tested have an asymmetric pattern of tangential deformation, which is of the order of  $10\ \mu\text{m}$ . Local fluid film thickness has been studied on a separate test rig. This rig employs a new method for distance measurements in the shaft/seal contact, based on an opto-electronic system as used in CD players. The preliminary results indicate that the investigated seal has a film thickness of the order of  $1\ \mu\text{m}$  under normal operational conditions, which is much higher than expected. Possible causes and improvements are discussed.

### 1. INTRODUCTION

Radial lip seals, also called rotating shaft seals, are very widely used machine elements, providing good performance at relatively low costs. They are employed to seal rotating and reciprocating shafts. They prevent (1) leakage of a fluid under low static pressure or that is splashed at the shaft, and (2) entrance of dust, dirt, etc., into the sealed fluid. The plain rotating shaft seal is the most interesting of the two, since the operational principles are still unclear. Figure 1 shows the configuration of a rotating shaft seal. The contact width is very narrow and of the order of  $0.1\ \text{mm}$ . The design of this modern lip seal is more than 60 years old.

In the ideal case, the geometry of a shaft seal is rotationally symmetric. Reynolds' equation explains that there is no reason why a continuous fluid film should develop, because it would be parallel. There is no entrainment action. Nevertheless, since 40 years researchers generally agree on the existence of a coherent fluid film, after Jagger (1957) concluded that the measured film thickness is of the order of  $1\ \mu\text{m}$ . More support for full film lubrication conditions stems from the exceptional low seal wear, after a run in period. During this run in period, which may take a few 100 hours, a wear track is formed. The surface roughness of this track is vital to the sealing properties (Horve 1991, 1992). The lubrication mechanism is not obvious and has not found general agreement yet.

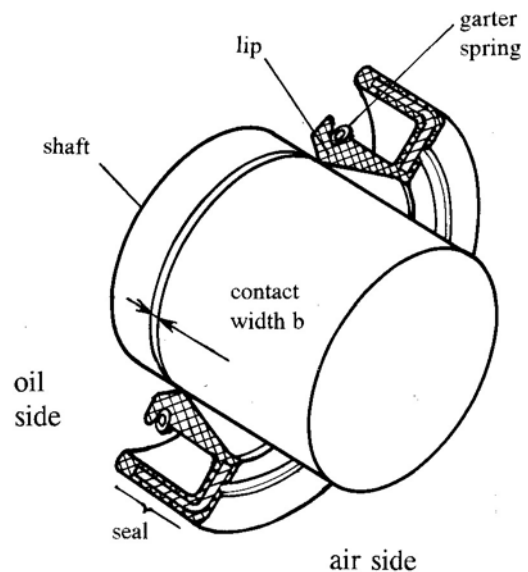


Figure 1: Plain radial lip seal for rotating shafts

If the existence of a full film is accepted, leakage would be expected. Fortunately, a properly operating plain lip seal does not leak after running in. Experienced seal designers know that a lip seal can pump fluid from the air side to the oil side, even

against a pressure head. This upstream pumping ability allows leakage free operation of the seal. The sealing mechanism is not obvious and still being disputed.

It is clear that experiments play an important role in the quest for the physical explanation of the lubrication and sealing mechanism. Most of the experimental studies on radial lip seals that have been published concern global quantities like friction torque, radial load, or leakage. As part of the solution lies in the surface roughness, these global measurements cannot solve the problem. Local measurements are needed to generate ideas for the understanding of the operating principles. This paper reports on local measurements of tangential deformations and of film thickness in the contact between shaft and seal, to provide more support for some recent theoretical models. A brief review of theories and experiments will be given first.

### 1.1. Notation

b	seal contact width	[m]
h	fluid film thickness	[m]
$h_{av}$	average value of film thickness	[m]
n	index of refraction	[-]
$p_{av}$	average contact pressure	[Nm <sup>-2</sup> ]
R	shaft radius	[m]
$T_f$	friction torque	[Nm]
y	axial position in contact zone	[m]
y=0	indicates contact edge at oil side	
$y_{max}$	indicates maximum tangential deformation	
$\eta$	dynamic fluid viscosity	[Nsm <sup>-2</sup> ]
$\omega$	shaft angular speed	[s <sup>-1</sup> ]

## 2. SEALING AND LUBRICATION

### 2.1. Theory

Many models have been suggested to explain the lubrication and sealing mechanism of rotating shaft seals in the past 40 years. Recent contributions to the theory with state of the art surveys of existing models can be found in Müller (1987), Stakenborg (1988), Salant and Flaherty (1995) and Van Bavel et al. (1996). From these references it can be concluded that fluid film formation can be explained by entrainment action, caused by deviations from a nominal smooth and parallel film. It is much more difficult to explain the sealing mechanism, however.

Kuzma (1969) was the first to present a radical departure from then existing sealing theories, by developing a concept based on tangential deformations of the seal surface due to viscous shear forces. He claims that his theory is applicable to lip seals too. The latest theories can explain both fluid film formation as well as upstream pumping by adopting this concept of tangential deformation (Salant and Flaherty (1995), Van Bavel et al. (1996)). These theories rely on the observations by Kammüller (1986), who found that the seal surface has a roughness texture, which is deformed in sliding (tangential) direction due to viscous shear stress. To yield upstream pumping, there is no need for an axial asymmetry in the static pressure distribution, but the tangential deformation should necessarily be axially asymmetric. The asperities in the contact now act like microvanes, which pump fluid, like in an asymmetric spiral groove bearing. Kammüller's work is discussed in more detail in section 2.2.1.

In the recent models it is assumed that the tangential deformation is inside the bulk material. Hence the asperities do not deform themselves, and the only interaction between them is caused by the hydrodynamic pressures. This implies that both new and run in seals should show the same tangential deformation pattern.

### 2.2. Experiments

Recent reviews on local measurement methods for seals can be found in Stakenborg (1988), Visscher and Kanters (1990), Visscher (1992), Poll and Gabelli (1992), and Poll et al. (1992). These measurements include tangential deformation, meniscus position, surface distance, fluid film thickness, film and surface temperature, lip motion, and static pressure. No pressures measurements under running conditions have been reported. In this section local measurements of tangential deformation and film thickness are briefly discussed.

#### 2.2.1. Tangential deformations

Kawahara et al. (1980) state that shear stresses will deform the lip surface in tangential direction. This deformation has an asymmetric distribution over the contact zone. Kawahara et al. (1980) only provided a schematic graph, and gave no experimental support, nor did they relate the deformations to pump flow. It was Kammüller (1986) who showed results of tangential deformation measurements, and related them to flow rates. Kammüller determined tangential

deformations of a 68 mm diameter seal surface at a shaft speed of about  $20 \text{ min}^{-1}$ , under supposedly full film regime conditions. Using light microscopy, he measured the distance of travel of a threshold between a highly reflecting layer of gold, evaporated on the lip, and the lip's elastomer. He documented 4 measurements. Two of them are reproduced in Figure 2.

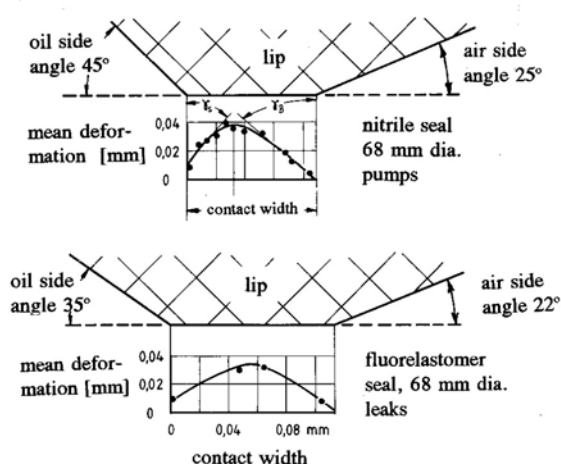


Figure 2: Tangential displacements of the seal surface in the contact zone, from Kammüller (1986).

This figure shows the averaged values of the deformation at two different circumferential positions. Only the relative deformations in the contact zone are of interest, not the bulk deformation of the lip, since the latter does not contribute to the pump flow. Kammüller plotted a few readings within the contact zone only. At the oil side a small offset appears. The maximum tangential displacement amounts to about  $40 \mu\text{m}$ , and the offset is roughly  $10 \mu\text{m}$ . These values are consistent with calculations by Salant and Flaherty (1995) and Van Bavel et al. (1996). In practice, the mechanical behaviour of a seal is not rotationally symmetric. So it can be anticipated that the tangential deformation will not be the same at different circumferential positions.

#### 2.2.2. The importance of seal surface roughness

Practice tells that some shaft surface roughness, somewhere in between  $0.2$  and  $0.8 \mu\text{m}$  (CLA), is

needed to create a properly run in seal surface. Kawahara and Hirabayashi (1979) found that, after running in, the sealing flow rate is determined by the seal surface roughness only. Nakamura and Kawahara (1984), Nakamura et al. (1985), and Nakamura (1987) concluded that the seal microgeometry is decisive for sealing. Horve (1991) showed that the seal surface roughness is of crucial importance for the pumping ability. Horve concluded that rough wear tracks, with an abundance of microasperities, give good sealing properties. On the other hand, smooth wear tracks with a few microasperities give poor sealing performance. It is clear that, to assess the effect of surface roughness on fluid film formation and on pump flow rate, local film thickness measurements are needed.

#### 2.2.3. Torque

Many authors interpret a Stribeck-like graph of friction torque vs. the so-called Gumbel number  $G (= \eta \omega / p_{av})$  for elastomer seals as if they were dealing with bearings. In the latter case, the friction minimum is associated with a transition from mixed to full film lubrication conditions, which can be proved by simple measurements (e.g., Ohmic resistance). The validity of this interpretation in lubricated elastomeric contact has never been demonstrated. Film pressures are usually low in elastomer contacts. If it is true that film thicknesses are very low (yielding very high shear stresses), high values of the coefficient of friction will result, which may be even higher than under unlubricated conditions. For example, the Gumbel number does not take into account any elastomer property, which may be of importance here. Van Leeuwen and Stakenborg (1990) performed a theoretical study and found a friction minimum under full film lubrication conditions. Experimental evidence can be found in Hoffmann et al. (1996). As a consequence, the lubrication condition cannot be determined by the friction behaviour alone. The film thickness is conclusive.

#### 2.2.4. Film thickness in lip seals

Film thickness can be deduced from global friction torque measurements or leakage flow, see Jagger (1957), but this can only serve as a check of the results. In the past, film thickness has been measured directly by means of electrical, magnetic,

and optical methods. These methods are briefly reviewed here.

Jagger (1957), Iny and Cameron (1961), and Schouten (1978) used the capacity of the oil film between the shaft and a specially treated lip seal. Film thickness was found to be of the order of 1  $\mu\text{m}$ . Kawahara et al. (1981) and Ogata et al. (1987) employ the Ohmic resistance between shaft and lip. The resistance measurement is used for determining the lubrication mode, hence for qualitative purposes only. The necessary seal treatment will change the mechanical properties and the roughness texture after running in.

A different approach is the measurement of the magnetic inductance between a shaft mounted sensor (a tape recorder head) and the seal with a magnetised fluid in between, by Poll and Gabelli (1992). The measured film thickness was of the same order as the capacitance measurements, 2 till 10  $\mu\text{m}$ , for a seal with very low small interference. The seal material remains unchanged.

Optical methods can also refrain from changes in the elastomer. McClune and Tabor (1978) found film thicknesses between a smooth rubber annulus and a glass disc lubricated with a special fluid by means of interferometry. Fluid film formation was attributed to intentional radial misalignment and of the order of 2  $\mu\text{m}$ . Poll et al. (1992) used fluorescent radiation in the contact between a hollow glass shaft and seal lubricated with a special fluid. The average film thickness does not markedly change with speed, and is about 0.35  $\mu\text{m}$ .

A new method, not applied before in film thickness measurements, is open loop focus error signal (fes) detection. This method was originally developed by Philips Research Laboratories for application in CD players. The potentials of fes detection in film thickness measurement are investigated by Visscher (1992), who also explains the principles (pp. 23-37)). He performed preliminary film thickness measurements on a cylindrical elastomer specimen and a flat glass plate, and concluded that the results were qualitatively in agreement with theory. See also Visscher and Struik (1994) and Visscher et al. (1994). The measured values of the film thickness were of the order of 10  $\mu\text{m}$ .

The focus error signal is a ratio of photodiode signals, and should therefore be more or less independent of the surface reflectance. Visscher claims that, in theory, surface roughness features are quantifiable by fes detection. The so-called radial error signal (res) is used for tracking purposes in CD players. Visscher shows that the res signal may be used to correct the fes signal for asperity slopes (Visscher (1992), pp. 35-36, 152-158). The spatial resolution of the fes measurement can be made very small: of the order of 1  $\mu\text{m}$  in a direction parallel to the fluid film, and of the order of 0.01  $\mu\text{m}$  in film thickness direction. It is therefore chosen to measure film thickness in radial lip seals.

It can be concluded that at present the film thickness in radial lip seals is not known to an accuracy which is desirable to assess the effects of surface roughness on their operation, and that the lubrication condition in a real shaft/seal system is not known either.

### 3. TEST EQUIPMENT

#### 3.1. Test specimens

Two brands of seals were used throughout the experiments, designated brand R and brand S. Brand R had a rough wear track, and brand S showed a smooth surface after running in. Data are given in the Appendix. Friction coefficients were also determined on a pin disc apparatus, where Shell Ondina 68 oil has been used under lubricated conditions. Each seal, of a total of 15, obtained 6 evaporated strips of about 1 mm width in groups of 3, the two groups 120° apart along the circumference, see also under 3.2.2. This allows comparisons for the rotational symmetry of the seal. In total 10 seals were run in, the remainder was in new (virgin) state. The seals investigated in this paper were run in on rig RLS1 (see below) at 1000  $\text{min}^{-1}$  during 25 up to 52 hours in Shell Tellus 46 oil. The steel shaft had a CLA surface roughness of about  $R_a \approx 0.5 \mu\text{m}$  in axial direction. The seals were cleaned three times in hexane before they were evaporated.

#### 3.2. Test rig RLS1

RLS1 is a universal seal test apparatus, used earlier by Schouten (1978) and Stakenborg (1988).

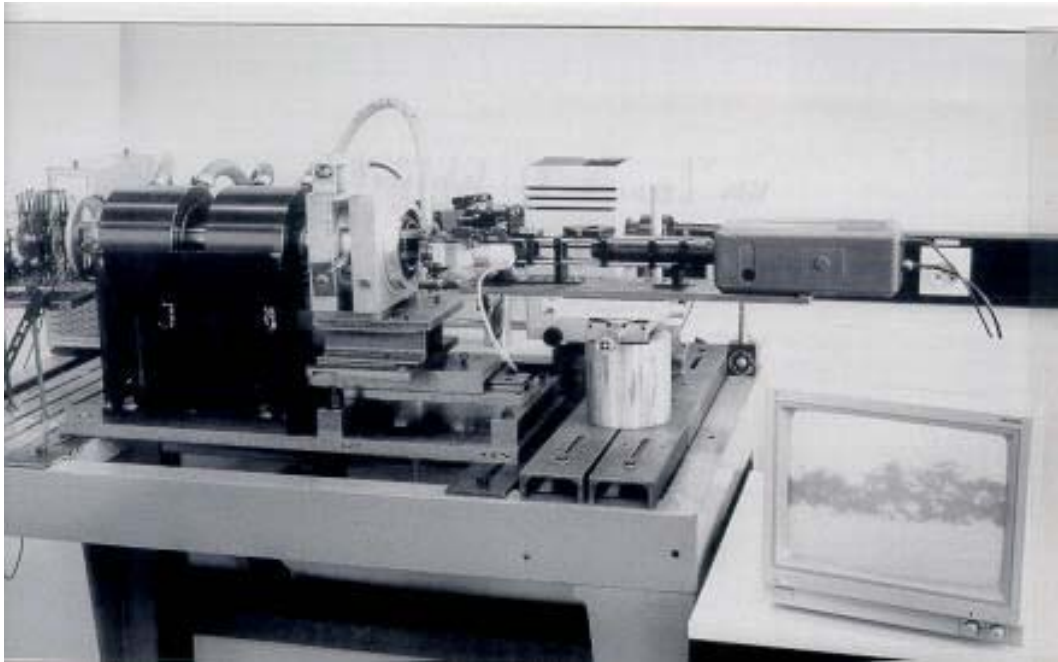


Figure 3: Photograph of the RLS1 test rig for optical measurements in the contact zone.

A picture of the arrangement is shown in Figure 3. Note the image on the monitor screen, which shows the contact zone of a seal of type R.

### 3.2.1. Description

The steel shaft is supported by two air bearings. At one end a hollow glass sleeve is fitted. The other side is connected to a motor by means of a low ratio transmission, allowing shaft speeds of the order of  $100 \mu\text{m/s}$ . At assembly the seal is slid over the glass shaft and mounted in a cylindrical housing, which is

supported on an air film, allowing torque measurements. To measure small displacements a long distance microscope was built, using a Spindler and Hoyer Microbench kit. The layout is given in Figure 4. The light is produced by a high pressure mercury source, and is filtered to obtain monochromatic light. For a sharp image with sufficient irradiance, an angle of incidence of  $90^\circ$  of the light rays on the seal surface was chosen. The images were taken in by a black and white videocamera and recorded on videocassette. A monitor and videoprinter were connected.

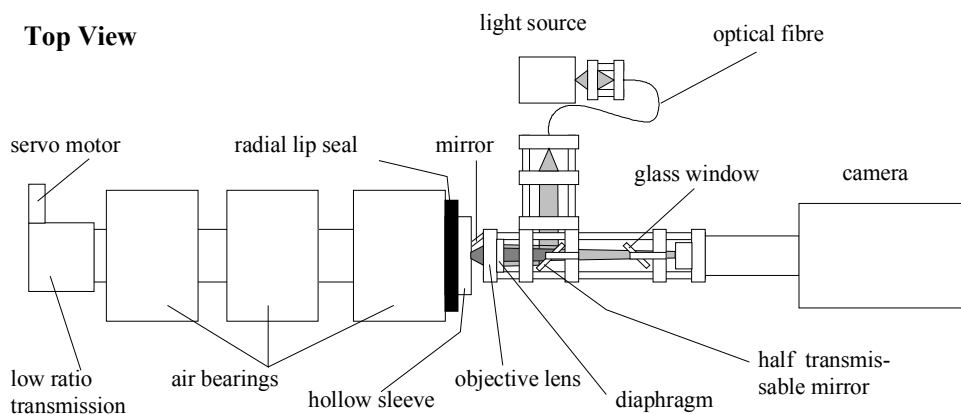


Figure 4: Layout of the modified test rig RLS1

The 70 mm diameter hollow shaft sleeve is made of BK7 glass, with a wall thickness of 4 mm. The radial runout of the sleeve is better than 0.01 mm. The CLA roughness is 0.04  $\mu\text{m}$ .

### 3.2.2. Test method

The seals were operated dry and at very low speeds. If the contact is lubricated, the difference between the oil and the contact zone is blurred. This is because the reflectance of the oil/glass interface is much closer to that of the elastomer/glass interface than the reflectance of the glass/air interface. It is assumed that the deformation state of the seal is the same under dry as under lubricated conditions. To simulate a lubricated state, it is needed to introduce permanent slip in the contact, so the seal will not stick to the glass shaft. Friction torque values under dry and under lubricated conditions were fairly close under low sliding speeds.

Essentially the method is based on distance measurement of moving markers. Several marker methods were tested: the border of an ink layer, of a vacuum evaporated layer, and speckles available in the contact zone. The ink layer was found to peel off easily. The number of useful speckles was only about 6 per image, which was considered too low. The edge between a highly reflecting layer and the low reflecting rubber marks a line, of which the deformation can be followed. This layer should be thin (not to affect the surface roughness) and narrow

(to have a low impact on the friction). Chromium layers were vacuum evaporated over the lip, with thickness  $< 400 \text{ \AA}$ . The chromium has a reflectance of 80%, the glass shaft will reflect about 4% at the glass/air interface, and the glass/rubber contact will reflect about 1%. Reflected light will therefore be white, grey, and black, respectively, and a sharp contrast between the contact and the glass/air interface results.

At first the coordinates of the undeformed and the deformed state were determined by hand from videoprints. The inaccuracy was  $\pm 5 \mu\text{m}$ , and could only be improved by repeating this tedious process many times for each print separately. In addition, this method depended on personal skills, which can lead to systematic errors and reproducibility errors. As the deformations are of the order of 10  $\mu\text{m}$ , a method with lower inaccuracy and independent of the executor has to be used.

Digital image analysis has less drawbacks. The videosignal (from the videocamera or VCR) is digitised by means of a PC equipped with a framegrabber and image processing software (TIM-win). Figure 5 shows two seal images. The smooth seal S has only a few microasperities, and therefore a smooth edge and a lip surface that is fitted tight to the shaft. On the contrary, the rough seal R has many asperities and many distinct contact spots, a very irregular contact edge, and a lip surface that does not fit close to the shaft.

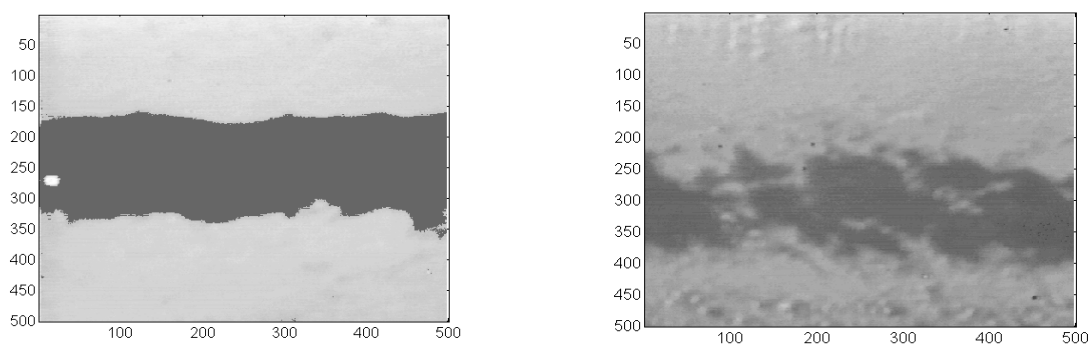


Figure 5: Images of the contact zone of a smooth seal S (left) and a rough seal R (right)

The data are arranged in a matrix and loaded into MATLAB. The Thresholding and Contour functions proved to be very convenient. A distinct speckle on the image of the seal served as a (moving) reference. In a MATLAB program the coordinates of initial contour lines are subtracted from coordinate values obtained under slip.

### 3.2.3. Calibration, reproducibility and inaccuracy

The magnification is determined by measuring a calibrated grid on the glass shaft. The transverse magnification factor was found to be about 300x. The video output signal showed that the image had a uniform irradiance distribution. The distribution is of utmost importance, while an intensity different from initial conditions necessitates a different value of the threshold, which would render a lower reliability. The inaccuracy of the method was determined by following the edge of the chromium layer on several seals, when the glass shaft sticks to the seal. In this case the relative deformation should

be zero. It was found that for the largest deformations the inaccuracy was better than  $\pm 2\mu\text{m}$ . If the same threshold value is chosen, and the initial adjustments are unchanged, the reproducibility is very good and independent of the person.

### 3.3. Test rig RLS2

Test rig RLS2 is a new apparatus, especially designed for film thickness determination in radial lip seals through fes detection.

#### 3.3.1. Description

The RLS2 apparatus consists of a hollow steel shaft, which holds a lens system and electronics, and is supported in two precision angle contact bearings. At one end a hollow glass sleeve is glued on this shaft. At the other side a pulley is mounted, which is driven by a toothed belt. The maximum shaft speed is  $600\text{ min}^{-1}$  and is closed loop controlled. Two seals are mounted in tandem geometry in a small housing, that can move axially with respect to the shaft.



Figure 6: Photograph of RLS 2 test rig for film thickness measurements (the test seal is removed). See text.



Measurement #	type of surface	distance to sleeve [mm]	reflectance [-]	sensitivity [mV/ $\mu$ m]
1	flat metal plate	2	20 %	570
2	polished metal plate	2	60 %	690
3	polished metal plate	0,1	60-80 %	630
4	flat NBR specimen	2	2 %	170
5	ring of NBR	<0,1	2 %	? unclear ?
6	ring of NBR with oil film	<0,1	<<1 %	20

Table 1: Sensitivity of the fes detection system with different specimens and variable object distance

Figure 6 shows the RLS2 test rig with the housing disassembled. The seal housing is mounted on a base plate with elastic pivots, allowing very small motions in two perpendicular directions. These motions are realised by means of two micrometers. At present, it is not possible to measure friction on this apparatus.

The hollow sleeve is made of duran glass with a refraction index  $n_s = 1.477$ . It is glued on the steel shaft. It has an outer diameter of 70h7 mm, and the thickness is 2.0 mm. The original sleeve had a radial runout of  $\pm 2 \mu\text{m}$ , but this one cracked (see under 5.2). The measurements reported in this paper were performed with a substitute that had a total runout of  $\pm 10 \mu\text{m}$  at the lens position. S type seals were used.

The lens system consists of a Philips GaAlAs laser, type CP065 (output 0.25 mW, laser wave length  $\lambda = 780 \text{ nm}$ ), an achromatic collimator lens with focal distance  $f = 20.0 \text{ mm}$ , and an aspherical objective lens with focal distance  $f = 9.0 \text{ mm}$ . The spot size is about  $3.5 \mu\text{m}$  in sliding direction, and the linearity range is  $\pm 13 \mu\text{m}$ . The laser light beam is reflected by the specimen, and diverted to 4 photodiodes by means of a beam splitter. The 4 diode signals are fed into an amplifier, built into the rotating shaft, which processes the diode signals to a low ohmic current. Brush contacts subsequently transmit the diode signals to a custom built instrumentation amplifier, that changes the diode signals into a focus error signal and a radial error signal. The sensitivity of the fes signal is about  $700 \text{ mV}/\mu\text{m}$  on a polished metal specimen in air.

With optical profilometry the unit is usually used in closed loop (autofocus) mode. This mode cannot be operated beyond 600 Hz due to mass inertia. If fluid film formation in radial lip seals is assumed to occur

at sliding speeds of at least 0.1 m/s, and a distance measurement at every  $10 \mu\text{m}$  is to be sampled at speeds of 1 m/s, a sampling frequency of at least 100 kHz will be necessary. In this case the optical system has to be run in open loop (fixed focus) mode, and the focus error signal is used for distance measurement. The maximum frequency of the amplifiers is 300 kHz.

### 3.3.2. Test method

The test rig was operated in a speed range between 0 and  $600 \text{ min}^{-1}$ . The oil used is a mix of Shell Ondina oils, and optically almost identical to the duran glass sleeve (see Visscher (1992), p. 150). The fes output signal is used for measuring the distance from the light spot, and the seal elastomer. If the outside of the glass sleeve is in focus, the fes signal equals zero. It is assumed that the fes output signal has the same sensitivity under dynamic conditions as under static conditions.

### 3.3.3. Calibration

The fes signal was calibrated on the rig by focusing the lens on a flat specimen, and lifting this specimen relative to the nonrotating shaft. This could easily be accomplished by adjusting one of the two micrometers. Different specimens were used for calibration, see Table 1.

It follows from measurement 1, 2, and 4 that the sensitivity of the fes signal decreases as the reflectance of the specimen decreases. If the specimen is closer to the shaft, reflection at the glass/air interface at the shaft outside will become more important, and now acts as a noise signal. Again, the sensitivity decreases (measurements 2 and 3). To

calibrate the fcs output on NBR seals, the lip of a seal was trimmed away, leaving a cylindrical ring of 70.2 mm inner diameter around the shaft. This NBR ring has a low reflectance, which results in a very low sensitivity at a very small distance of less than 0.1 mm. Presumably the reflected light from the rubber interferes with the reflected light from the glass/air interface. If the space between shaft and a NBR ring is filled with the Ondina oil, the sensitivity decreases to 0.020 V/ $\mu\text{m}$ . This is consistent with Visscher (1992, p. 61).

#### 4. MEASUREMENT RESULTS

##### 4.1. Tangential deformations (RLS1)

Not all chromium layers adhered equally well on the elastomer surface. The accessibility to the seal's tip is difficult. In addition, adhesion depends on the substrate roughness and the cleanliness. Oil rests will remain on the seal, even after thorough cleaning. The chromium layer sticks better to seal S than to seal R. A few seals were not useful, because the chromium came off too easily, or the tip of the

lip had no chromium deposit at all, or the chromium would peel off under continuous shear. Another problem arising with rough seals is the variation of the real contact area during shaft rotation. If a contact spot comes loose, light will be reflected at the glass/air instead of the glass/elastomer interface. This results in a local increase of the reflectance, obscuring the elastomer valley under it, and making the measurement unreliable. For these reasons most results were obtained on smooth seals

Figure 7 shows some results. The oil side is at the left, the air side at the right. Figure 7b presents the tangential deformation under the no slip (stick) condition, see also under 3.2.3. Figure 7c and 7d show the tangential deformation on a new seal S8, at two distinct circumferential positions. In Figure 7e and 7f two graphs are shown of a run in rough seal R4, again at two separate positions along the circumference.

From observations of the monitor screen it follows that the axial position of the contact zone varies along the circumference, but the contact width is almost constant. This is also corroborated by the graphs from Figure 7c - 7f. Running in (at least until 50 hours at 1000  $\text{min}^{-1}$ ), does not significantly change the contact width nor the tangential deflections. The contact width is found to be in between 0.037 mm and 0.065 mm.

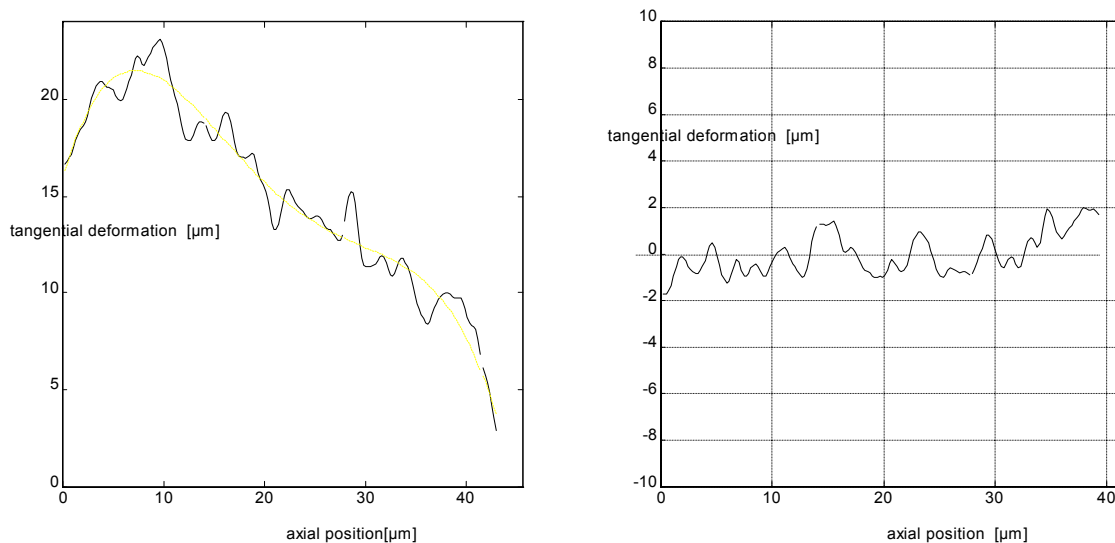


Figure 7: Tangential deformation of seals. The oil side is at the left. S = smooth, R = rough. (a) run in smooth seal S3, (b) run in smooth seal S3 under stick conditions

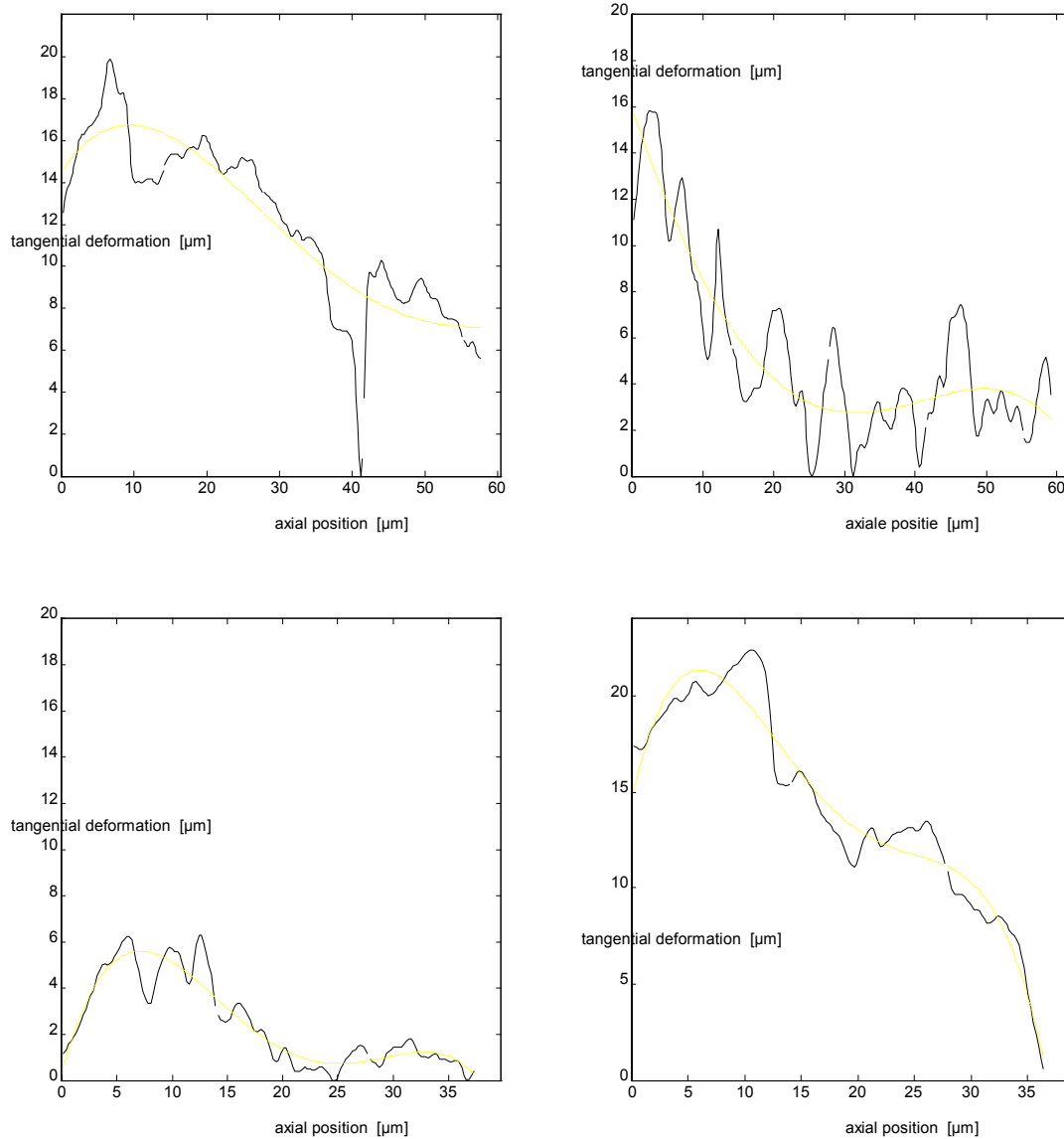


Figure 7 (cont.): (c) new smooth seal S8.1, (d) new smooth seal S8.2, at  $120^\circ$  from (c)  
(e) run in rough seal R4.1, (f) run in rough seal R4.2, at  $120^\circ$  from (e)

The maximum tangential deformation is in between 6 and 20  $\mu\text{m}$ . This maximum occurs at a position in between 0 and 30% of contact width  $b$  from the oil side edge, with a mean of about  $y_{\text{max}} \approx 0.2b$ . The tangential deformation has an offset in sliding direction at the oil side, which is between 1 and 15  $\mu\text{m}$ . At different circumferential positions the deformation pattern can differ considerably.

#### 4.2. Film thickness (RLS2)

The first results obtained on RLS2 give an impression of the potentials of open loop fes detection for film thickness measurement in elastomer seals. The low reflectance of the elastomer complicates the focusing on the outside of the shaft so much that the fes signal could not be set zero. Figure 8 shows the fes signal expressed in  $\mu\text{m}$  for  $6 \text{ min}^{-1}$  and for  $600 \text{ min}^{-1}$ .

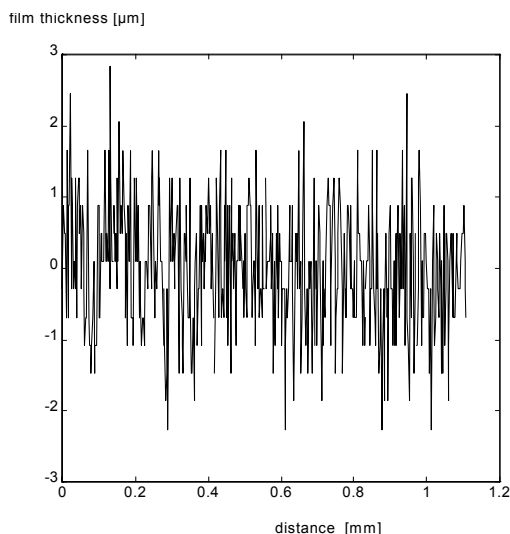


Figure 8a: Film thickness measurement for  $6 \text{ min}^{-1}$

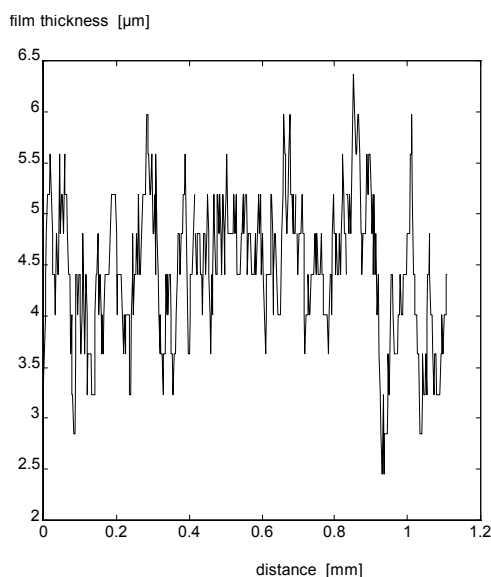


Figure 8b: Film thickness measurement for  $600 \text{ min}^{-1}$

It appears that the fes signal contains very steep gradients, originating from noise. The noise level is about 40 mV, which corresponds to 2  $\mu\text{m}$  film thickness. The autopower spectrum of the noise signal (with nonrotating shaft) contains frequencies in a wide band ranging far over 100 kHz. The highest amplitudes occur below 60 kHz. Earlier (in section 3.3.1) it was concluded that frequencies of the order of at least 100 kHz could be of interest for roughness effects. Hence it is not functional to filter the noise.

## 5. DISCUSSION

### 5.1 Tangential deformations in the contact zone (RLS1)

#### 5.1.1. Tangential deformations

Some results show very sharp gradients in the deformation, which cannot originate from shear stresses. See, e.g., Figure 7c. Sharp peaks may be ascribed to imperfect adhesion of the chromium layer. Due to shear stresses the deposited layer may come loose, in which case it is transported along a longer distance than when it would adhere perfectly to the seal surface. Sharp craters could originate from valleys in the surface texture. Valleys are not in contact with the glass shaft. They are only moved because the surrounding asperity peaks, which are in contact, force them to do so. The valleys may lag behind, and have less deformation. Thus the measured distribution cannot be smooth.

The offset at the oil side is evident, and amounts 16 till 100 % of the maximum tangential deformation. Van Bavel et al. (1996) have assumed an offset of 25 % of a presumed maximum deformation of 10  $\mu\text{m}$ , and found an increase of at least 2 orders of magnitude in pump rate compared to zero offset (Ruijl (1994)). Salant and Flaherty (1995) calculated an offset of 25 till 30 % of a maximum displacement of 70 till 80  $\mu\text{m}$  for a surface covered with microasperities. Therefore this offset seems essential for sealing.

The tangential deformation is not uniform along the circumference of the same seal. This can be attributed to seal imperfections (in material and geometry), causing deviations from rotatory symmetry. This implies that areas having large deformation are followed by zones with low deformation. In other words: areas with a high reverse pump rate are succeeded by zones with a low (or even negative) pump rate. For a well operating seal, fluid that is accidentally leaked to the air side in a certain zone, will be pumped back into the oil side at another zone.

It is not possible to distinguish the tangential deformation of run in seals from that of new ones. This suggests that, on the whole, the tangential deformation is independent of the surface roughness texture. Hence, tangential deformations are determined by the bulk of the lip rather than by the surface roughness..

The influence of time on the deflection could not be measured. Due to wear of the chromium layer the threshold value had to be adjusted continuously. This is unacceptable, see section 3.2.3. Initial experiments, using videoprints, indicate that an almost uniform displacement is added to the existing deformation in time. Hence the deformation distribution does not change substantially.

### 5.1.2. Contact width

The contact width of a new seal appears to be about 0.060 mm. This is in line with FEM analysis results of Stakenborg (1988), who calculated  $b = 0.073$  mm for this shaft/seal combination. It is also supported by calculations by Sponagel et al. (1987) for the same seal and shaft size ( $b = 0.080$  mm), and by experiments of Nakamura and Kawahara (1984) and Nakamura (1987), who find contact widths of run in seals with 85 mm diameter in between 0.050 and 0.100 mm.

Even after running in, this narrow contact band will not become markedly wider. Thus the static contact pressure distribution will not change considerably, and maintain the same average value. This is remarkable, since Gabelli et al. (1992) came to opposite conclusions. They calculated a contact width of about  $b \approx 0.150$  mm for a new 110 mm diameter seal, and  $b \approx 0.400$  mm for a run in seal. Consequently, their average static contact pressure drops correspondingly.

It follows that the contact width and the wear track width can differ notably. During running in the width of the wear track increases with time. In a different series of experiments on RLS1, the wear track width was found to be in between 0.050 and 0.30 mm for smooth seals S, for running times between 5 minutes and 50 hours. Shaft motions (bending, radial runout) result in an axial translation and in rotation of the seal lip with respect to the shaft, yielding a wear track that is wider than the contact width. Gawlinski and Konderla (1984) did a FEM analysis of the seal dynamics and found that the contact width varied a factor of almost 2 during a shaft revolution. Seal geometry and assembly imperfections will only increase this difference and render an even wider running track on the shaft.

## 5.2 Film thickness (RLS2)

### 5.2.1. Film thickness values

If fluid film formation can be neglected at a speed as low as  $6 \text{ min}^{-1}$ , this speed could serve as a reference for zero film thickness. The  $f_{es}$  signal was determined at several shaft speeds, at the same part of the seal circumference (constant sampling length of 1.1 mm), and centre line averaged. Subsequently, 5 measurements were done at each speed and the average of these 5 was determined ( $h_{av}$ ). The value of  $h_{av,6}$  at  $6 \text{ min}^{-1}$  was set equal to zero, and the other readings were corrected correspondingly. This results in Figure 9.

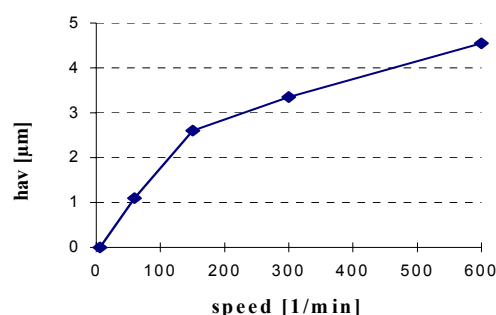


Figure 9: Averaged film thickness values vs. speed

Figure 9 suggests that film thickness increases with speed, as in a hydrodynamic bearing, and amounts up to  $4.5 \mu\text{m}$  at  $600 \text{ min}^{-1}$ . A simple Petroff model for the friction torque of the parallel smooth seal, see Jagger (1957)), yields

$$h_{av} \approx \{(2\pi \eta \omega b R^3)/T_f\}$$

for the average film thickness  $h_{av}$ , where  $T_f$  represents the friction torque. If it is assumed that at  $\eta = 0.01 \text{ Pa}\cdot\text{s}$  (at 333 K),  $\omega = 600 \text{ min}^{-1} = 62.8 \text{ s}^{-1}$ ,  $b = 2 \cdot 10^{-4} \text{ m}$ ,  $R = 35 \cdot 10^{-3} \text{ m}$ ,  $T_f = 0.8 \text{ Nm}$ , it is found that  $h_{av} \approx 0.04 \mu\text{m}$ . Therefore, it may be concluded that the measured averaged film thickness is about 2 orders of magnitude higher than expected. In addition, the signal to noise ratio is too low.

The first glass sleeve cracked during operation, see also section 3.3.1. An analysis of the temperature rise in a simple geometrical model was undertaken with MARC FE software. If it is assumed that one seal dissipates  $60 \text{ W}$  at  $600 \text{ min}^{-1}$ , and that, far away from the contact, the oil has attained a temperature of 303 K, and the air of 293 K, a maximum contact temperature of 630 K can be attained. These high temperatures can be reached in a few seconds. Therefore, high thermal stresses are created in the glass sleeve. At lower speeds the temperature rise is less dramatic: 470 K at  $300 \text{ min}^{-1}$ , 385 K at  $150 \text{ min}^{-1}$ ,

335 K at 60 min<sup>-1</sup>, and 306 K at 6 min<sup>-1</sup>. If, e.g., a sapphire sleeve had been used, the maximum contact temperature at 600 min<sup>-1</sup> would have been 318 K.

A substantial temperature rise has a large impact on the film thickness measurement, see Visscher (1992) pp. 217-229. Depending on the actual temperatures, an over as well as an underestimation of the film thickness is possible. If the temperature of the lubricant is 413 K, of the shaft 393 K, and of the lens system 303 K, respectively, the film thickness will be overestimated by about 4 µm. The influence of pressure on the film thickness measurement is less than 0.15 µm. It follows that the measured behaviour of film thickness with speed may be mainly attributed to temperature effects. Several corrective measures to compensate for these effects are conceivable.

It is clear that in test rig RLS2 the accuracy of fes detection is affected considerably by temperature, and therefore the temperature should be kept under control.

#### 5.2.2. Noise

Reflectances can be estimated by measuring the laser diode signals under various conditions. It is concluded that the reflectance of the oil/elastomer interface is about 0.4 %, and that the internal reflectance in the sensor unit amounts approximately 0.8 %. In this respect the reflectance on the shaft inside (air/glass interface) can be neglected. See also under 3.3.3.

Visscher (1992, pp. 189-190), in discussing the noise problem, concludes that the signal level should be increased. He suggests a laser source with higher light intensity and a thin metallic coating on the seal. Other feasible improvements are a decrease in the internal sensor reflectance and the use of a high refraction index glass shaft. If glass with an index of refraction of  $n = 1.7$  is used, the reflection on the oil/elastomer surface rises from 0.4 % to 1.8 %.

What is considered as noise could partly originate from asperity slopes. The effect of slopes on the fes signal can be accounted for by using the res signal, see under 2.2.4. As the surface slopes are statistically distributed over the seal contact, their influence on the fes signal may be disguised as noise. The RMS roughness of the tested seals amounts 1 - 2.5 µm. Considering the wave length scale of about 10 µm, this results in steep slopes of far over 0.1 (for a dismounted seal). This should be further explored.

## 6. CONCLUSIONS

- (1) On the whole, Kammüller's hypothesis of an asymmetric tangential deformation distribution is corroborated by the experiments on RLS1.
- (2) The tangential deformations are not constant along the circumference.
- (3) The tangential deformation is determined by the bulk of the lip and not by the roughness texture.
- (4) New and run in seals both show the same tangential deformation pattern.
- (5) The contact width does hardly change under operation and is obviously smaller than the wear track width.
- (6) The reflectance on the oil/elastomer interface on test rig RLS2 is about 0.4 %. The sensitivity of the fes signal in an oil lubricated seal amounts about 20 mV/µm. This is considered sufficient for fes measurements.
- (7) The S/N ratio of the fes signal on the current RLS2 rig is too low. Corrective measures are suggested.
- (8) The poor conductance of the glass sleeve introduces high contact temperatures, which result in a considerable overestimation of the film thickness. Different materials, like sapphire, should be considered.

## 7. ACKNOWLEDGEMENTS

The authors gratefully acknowledge the support of, and stimulating discussions with Prof. E.A. Muijderman and Mr. P.G.M. van Bavel, the technical skills of Mr. J.A. Peels, the help of student Mr. W.A. Monden, the advice of Messrs. C. van der Laan, K.G. Struik and R. Petterson, and the Central Technical Services of the University, for designing and building RLS2.

## REFERENCES

- van Bavel, P.G.M. et al., 1996, *Trans. ASME, J.o.Tribology*, Vol. 118, pp. 266-275
- Gabelli, A., et al., 1992, in: *Fluid Sealing*, by B.S. Nau (ed.), Kluwer, Dordrecht, pp. 21-39
- Gawlinski, M.J., and Konderla, P., 1984, in: *Proceedings 10th Int. Conf. on Fluid Sealing*, BHRA, Cranfield, pp. 139-155
- Hoffmann, C., et al., 1996, *Konstruktion*, Vol. 48, pp. 94-98
- Horve, L., 1991, *SAE Paper*, No. 910530, 8 pp.
- Horve, L.A., 1992, in: *Fluid Sealing*, by B.S. Nau (ed.), Kluwer, Dordrecht, pp. 5-19
- Iny, E.H., and Cameron, A., 1961, *Proc. 1st Int. Conf. on Fluid Sealing*, BHRA, Barlow, Paper A2, 15 pp.
- Jagger, E.T., 1957, *Proc. Conf. on Lubrication and Wear*, I.Mech.E., London, Paper 93, pp. 409-415
- Kammüller, M., 1986, "On the sealing action of rotating shaft seals" (in German), *Ph.D. Thesis*, Stuttgart University, pp. 49-59
- Kawahara, Y., and Hirabayashi, H., 1979, *ASLE Trans.*, Vol. 22, pp. 46-55
- Kawahara, Y., et al. 1980, *ASLE Trans.*, Vol. 23, pp. 93-102
- Kawahara, Y., et al. 1981, in: *Proceedings 9th Int. Conf. on Fluid Sealing*, pp. 73-85
- Kuzma, D.C., 1969, in: *Proceedings 4th Int. Conf. on Fluid Sealing*, BHRA, Cranfield, Paper 18, pp. 165 - 173
- van Leeuwen, H.J., and Stakenborg, M.J.L., 1990, *Trans. ASME, J.o.Tribology*, Vol. 112, pp. 584-592
- McClune, C.R., and Tabor, D., 1978, *Tribology International*, Vol. 11, pp. 219-227
- Müller, H.K., 1987, in: *Proc. 11th. Conf. on Fluid Sealing*, Elsevier, London, pp. 698-709
- Nakamura, K., and Kawahara, Y., 1984, in: *Proceedings 10th Int. Conf. on Fluid Sealing*, BHRA, Cranfield, pp. 87-105
- Nakamura, K., et al., 1985, in: *Proc. JSLE Int. Trib. Conf.*, Elsevier, Amsterdam, pp. 805-810
- Nakamura, K., 1987, *Tribology International*, Vol. 20, No. 2, pp. 90-101
- Ogata, M., et al., 1987, in: *Fluid Film Lubrication - Osborne Reynolds Centenary*, by D. Dowson, et al. (eds.), Elsevier, Amsterdam, pp. 553 - 560
- Poll, G., and Gabelli, A., 1992, *Trans. ASME, J.o.Tribology*, Vol. 114, pp. 290 - 297
- Poll, G., et al., 1992, in: *Fluid Sealing*, by B.S. Nau (ed.), Kluwer, Dordrecht, pp. 55-77
- Ruijl, T.A.M., "Theoretical concept of the pumping effect of radial lip seals" (in Dutch), *M.Sc. Thesis*, Eindhoven University of Technology, 68 pp.
- Salant, R.F., and Flaherty, A.L., 1995, *Trans. ASME, J.o.Tribology*, Vol. 117, pp. 53-59
- Schouten, M.J.W., 1978, *FKM-Heft*, No.72, Maschinenbau Verlag Frankfurt, pp. 45-56
- Sponagel, S., et al., 1987, in: *Proc. 11th. Conf. on Fluid Sealing*, by B.S. Nau (ed.), Elsevier, London, pp. 748-772
- Stakenborg, M.J.L., 1988, "On the sealing and lubrication mechanism of radial lip seals", *Ph.D. Thesis*, Eindhoven University of Technology, 92 pp.
- Visscher, M., and Kanters, A.F.C., 1990, *Lub. Engng.*, Vol. 44, pp. 785-191
- Visscher, M., 1992, "The measurement of the film thickness and the roughness deformation of lubricated elastomers", *Ph.D. Thesis*, Eindhoven University of Technology, 249 pp.
- Visscher, M., and Struik, K.G., 1994, *Precision Engineering*, Vol. 16, pp. 192 - 198.
- Visscher, M., et al., 1994, *Precision Engineering*, Vol. 16, pp. 199 - 204.

## A. Data of seals R and S

*Seal R (rough wear track)*

material: NBR (nitrile)  
 size: 70x100x10 mm  
 inner diameter  $68.5 \times 10^{-3}$  m  
 garter spring stiffness 0.062 N/m  
 initial spring force 1.920 N  
 coefficient of friction (on pin and disc):  
     dry 0.7-0.75, speeds up to 0.03 m/s  
     lubricated 0.6-0.2, speeds up to 0.16 m/s  
 index of refraction  $n = 1.30$

*Seal S (smooth wear track)*

material: NBR (nitrile)  
 size: 70x100x10 mm  
 inner diameter  $68.6 \times 10^{-3}$  m  
 garter spring stiffness 0.095 N/m  
 initial spring force 1.911 N  
 coefficient of friction (on pin and disc):  
     dry 0.3-0.65, speeds up to 0.03 m/s  
     lubricated 0.6-0.2, speeds up to 0.16 m/s  
 index of refraction  $n = 1.30$